

# Searching for a possible dipole anisotropy in acceleration scale with 147 rotationally supported galaxies<sup>\*</sup>

Zhe Chang(常哲)<sup>1,2</sup> Hai-Nan Lin(林海南)<sup>3</sup> Zhi-Chao Zhao(赵志超)<sup>1,2</sup> Yong Zhou(周勇)<sup>1,2;1)</sup>

<sup>1</sup> Institute of High Energy Physics, Chinese Academy of Sciences, Beijing 100049, China

<sup>2</sup> School of Physical Sciences, University of Chinese Academy of Sciences, Beijing 100049, China

<sup>3</sup> Department of Physics, Chongqing University, Chongqing 401331, China

**Abstract:** We report a possible dipole anisotropy in acceleration scale  $g_{\uparrow}$  with 147 rotationally supported galaxies in the local Universe. It is found that a monopole and dipole correction for the radial acceleration relation can better describe the SPARC data set. The monopole term is negligible but the dipole magnitude is significant. It is also found that the dipole correction is mostly induced by anisotropy in the acceleration scale. The magnitude of the  $\hat{g}_{\uparrow}$ -dipole reaches  $0.25 \pm 0.04$ , and its direction is aligned to  $(l, b) = (171.30^\circ \pm 7.18^\circ, -15.41^\circ \pm 4.87^\circ)$ , which is very close to the maximum anisotropy direction from the hemisphere comparison method. Furthermore, a robust check shows that the dipole anisotropy could not be reproduced by an isotropic mock data set. However, it is still premature to claim that the Universe is anisotropic, due to the small data samples and uncertainty in the current observations.

**Keywords:** galaxies: kinematics and dynamics, galaxies: fundamental parameters, large-scale structure of Universe

**PACS:** 98.62.Ck, 98.62.Dm, 98.80.k **DOI:** 10.1088/1674-1137/42/11/115103

## 1 Introduction

One of the foundations of the standard cosmological paradigm ( $\Lambda$ CDM) is the so-called cosmological principle, which states that the Universe is homogeneous and isotropic at large scales [1]. This principle is in accordance with most cosmological observations, especially with the approximate isotropy of the cosmic microwave background (CMB) radiation from the Wilkinson Microwave Anisotropy Probe (WMAP) [2, 3] and Planck satellites [4, 5]. However, there still exist some cosmological observations that challenge the cosmological principle. These include the large-scale alignments of quasar polarization vectors [6], the unexpected large-scale bulk flow [7, 8], the spatial variation of the fine structure constant [9, 10], and the dipole of supernova distance modulus [11–14]. All of these facts hint that the Universe may be anisotropic to some extent.

On the galactic scale, the mass discrepancy problem [15, 16] has been known for many years. The observed gravitational potential cannot be explained by the luminous matter (stellar and gas). Hence, it seems that there is a significant amount of non-luminous matter is needed, i.e. dark matter. To date, however, no direct evidence of the existence of dark matter has been found [17, 18].

A successful alternative to the dark matter hypothesis is the modified Newtonian dynamics (MOND) [19], which attributes the mass discrepancies in galactic systems to a departure from standard dynamics at low accelerations.

In principle, the MOND theory assumes a universal constant acceleration scale for all galaxies [19–21]. In practice, however, the acceleration scale is considered as a free parameter to fit the galaxy rotation curve, and different galaxies may have different acceleration scales [22–24]. Milgrom [25] also suggested that the acceleration scale may be a fingerprint of cosmology on local dynamics and related to the Hubble constant. Therefore, cosmological anisotropy at large scales may imprint on the acceleration scale in the local Universe. These ideas inspire us to investigate the possibility of spatial anisotropy in the acceleration scale. In our previous work [26], by making use of the hemisphere comparison method to search for such an anisotropy from the SPARC data set, we found that the maximum anisotropy level is significant and reaches up to  $0.37 \pm 0.04$  in the direction  $(l, b) = (175.5_{-10}^{+6}, -6.5_{-3}^{+9})$ . In this paper, we search for a monopole and dipole correction for the radial acceleration relation, and try to find the possible anisotropy from the SPARC data set.

Received 27 July 2018, Published online 25 September 2018

<sup>\*</sup> Supported by National Natural Science Foundation of China (11675182, 11690022, 11603005)

1) E-mail: zhoyong@ihep.ac.cn

©2018 Chinese Physical Society and the Institute of High Energy Physics of the Chinese Academy of Sciences and the Institute of Modern Physics of the Chinese Academy of Sciences and IOP Publishing Ltd

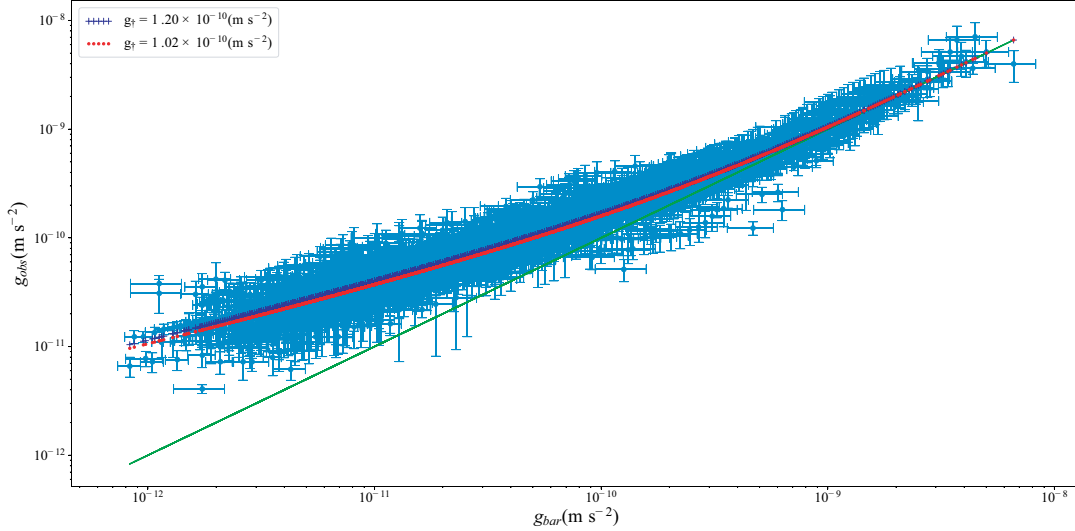


Fig. 1. (color online) The radial acceleration relation between the centripetal acceleration  $g_{\text{obs}}$  and the baryonic acceleration  $g_{\text{bar}}$  for all 2693 data points in 147 galaxies. The two dotted lines correspond to the fitting curve ( $g_{\dagger} = 1.20 \times 10^{-10} \text{ m s}^{-2}$ ) in McGaugh et al. [29] and our fitting curve ( $g_{\dagger} = 1.02 \times 10^{-10} \text{ m s}^{-2}$ ), respectively. The solid line is the line of unity.

The rest of this paper is organized as follows. In Section 2, we give a brief introduction to the SPARC data set and the radial acceleration relation. In Section 3, we show a monopole and dipole correction for the radial acceleration relation by making use of the Markov chain Monte Carlo (MCMC) method to explore the entire parameter space. The information criterion (IC) is used for model comparison. In Section 4, the MCMC results for whole parameter spaces are analyzed, and we compare the dipole anisotropy and the goodness of fit for different dipole models. We also compare the possible dipole anisotropy with the hemisphere anisotropy in our previous work [26]. In Section 5, we make a robust check to examine whether the dipole anisotropy could be reproduced by a statistically isotropic data set. Finally, conclusions and discussion are given in Section 6.

## 2 Data and radial acceleration relation

We employ the new Spitzer Photometry and Accurate Rotation Curves (SPARC) data set [27, 28]. The SPARC data set is a sample of 175 disk galaxies with new surface photometry at  $3.6 \mu\text{m}$  and high-quality rotation curves from previous HI/H $\alpha$  studies. For investigating the radial acceleration relation, McGaugh et al. [29] have adopted a few modest quality criteria to exclude some unreliable data. Finally, a sample of 2693 data points in 147 galaxies have been left. Here we use the same sample to search for the possible spatial dipole anisotropy. The SPARC data set does not include the galactic coordinate. We complete it for each galaxy from previous studies [30, 31] and by retrieving the NED dataset [32].

McGaugh et al. [29] obtained a fitting function that describes the radial acceleration relation well for all 2693 data points. The fitting function is of the form

$$g_{\text{obs}} = \frac{g_{\text{bar}}}{1 - e^{-\sqrt{g_{\text{bar}}/g_{\dagger}}}}, \quad (1)$$

where  $g_{\text{bar}}$  is the baryonic (gravitational) acceleration predicted by the distribution of baryonic mass and  $g_{\text{obs}}$  is the observed dynamic centripetal acceleration traced by rotation curves. The function has a unique fitting parameter  $g_{\dagger}$ , which corresponds to the MOND acceleration scale. They found  $g_{\dagger} = [1.20 \pm 0.02 \text{ (random)} \pm 0.24 \text{ (systematic)}] \times 10^{-10} \text{ m s}^{-2}$ . This value is consistent with that predicted by the MOND theory [19, 33]. The MOND theory also predicts two limiting cases for the radial acceleration relation. In the deep-MOND limit, i.e.  $g_{\text{bar}} \ll g_{\dagger}$ , the fitting function (1) becomes  $g_{\text{obs}} \approx \sqrt{g_{\text{bar}}g_{\dagger}}$ , where the mass discrepancy appears. In the Newtonian limit, i.e.  $g_{\text{bar}} \gg g_{\dagger}$ , the fitting function (1) becomes  $g_{\text{obs}} \approx g_{\text{bar}}$  and Newtonian dynamics is recovered. The radial acceleration relation and the SPARC data points are illustrated in Fig. 1.

## 3 Methodology

### 3.1 Fitting method

The same as McGaugh et al. [29], we make use of the orthogonal-distance-regression (ODR) algorithm [34] to fit the radial acceleration relation. The advantage of this method is that it can consider errors on both variables.

The chi-squared is defined as

$$\chi^2 = \sum_{i=1}^n \frac{[g_{\text{th}}(g_{\text{bar},i} + \delta_i, g_{\dagger}) - g_{\text{obs},i}]^2}{\sigma_{\text{obs},i}^2} + \frac{\delta_i^2}{\sigma_{\text{bar},i}^2}, \quad (2)$$

where  $\sigma_{\text{obs}}$  and  $\sigma_{\text{bar}}$  are the uncertainty of  $g_{\text{obs}}$  and  $g_{\text{bar}}$ , respectively. The total number of data points is  $n=2693$ .  $\delta_i$  is an interim parameter which is used for finding out the weighted orthogonal (shortest) distance from the curve  $g_{\text{th}}(g_{\text{bar}}, g_{\dagger})$  to the  $i$ th data point. The curve is same as the right-hand side of Eq. (1), i.e.

$$g_{\text{th}}(g_{\text{bar}}, g_{\dagger}) = \frac{g_{\text{bar}}}{1 - e^{-\sqrt{g_{\text{bar}}/g_{\dagger}}}}, \quad (3)$$

where  $g_{\text{th}}$  represents the theoretical centripetal acceleration. Therefore, the chi-squared (2) is the sum of the squares of the weighted orthogonal distances from the curve to the  $n$  data points. Eventually, we minimize the chi-squared to find the best-fit value of  $g_{\dagger}$ . We repeat the fitting process used by McGaugh et al. [29] and reproduce the same result, if the logarithmic distance (base 10) of the first term in the chi-squared (2) is taken. For the original form of chi-squared (2), we find the best-fit value for the universal acceleration scale is  $g_{\dagger} = (1.02 \pm 0.02) \times 10^{-10} \text{ m s}^{-2}$ , which corresponds to the unnormalized chi-squared  $\chi^2 = 4020$ . This fitting curve is also plotted in Fig. 1. It is worth noting that the difference in the best-fit value comes from the form of the first term in the chi-squared (2), which could only have a slight impact on the possible dipole anisotropy. What we are concerned with here is the relative variation of the acceleration scale in different directions, which is similar to the hemisphere anisotropy.

### 3.2 Monopole and dipole corrections

The MOND theory assumes a universal constant acceleration scale for all galaxies [19–21]. However, the acceleration scale has been found to vary from galaxy to galaxy [22–24]. In our previous work [26], we found that there exists a hemisphere anisotropy in acceleration scale in the SPARC data set. In this paper, we show a monopole and dipole correction for the radial acceleration relation to search for a possible spatial dipole anisotropy in the local Universe. The monopole and dipole correction is a commonly used method to search for possible dipole anisotropy, for instance, the spatial variation of the fine structure constant [9, 10], and the dipole modulation of supernova distance modulus [11–14]. Here, we first assume the dipole anisotropy comes from the radial acceleration. The theoretical centripetal acceleration with a monopole and dipole correction is of the form

$$\hat{g}_{\text{th}}(g_{\text{bar}}, g_{\dagger}) = g_{\text{th}}(g_{\text{bar}}, g_{\dagger}) [1 + A + B \hat{\mathbf{m}} \cdot \hat{\mathbf{p}}], \quad (4)$$

where the acceleration scale has been fixed at the best-fit value  $g_{\dagger} = 1.02 \times 10^{-10} \text{ m s}^{-2}$ .  $A$  and  $B$  are the

monopole term and dipole magnitude, respectively.  $\hat{\mathbf{m}}$  and  $\hat{\mathbf{p}}$  are unit vectors pointing towards the dipole direction and galaxy position, respectively. In galactic coordinates, the dipole direction can be represented as  $\hat{\mathbf{m}} = \cos(b) \cos(l) \hat{\mathbf{i}} + \cos(b) \sin(l) \hat{\mathbf{j}} + \sin(b) \hat{\mathbf{k}}$ , where  $l$  and  $b$  are galactic longitude and latitude, respectively. Similarly, the position of the  $i$ th galaxy can be represented as  $\hat{\mathbf{p}}_i = \cos(b_i) \cos(l_i) \hat{\mathbf{i}} + \cos(b_i) \sin(l_i) \hat{\mathbf{j}} + \sin(b_i) \hat{\mathbf{k}}$ . Then we use the corrected theoretical centripetal acceleration  $\hat{g}_{\text{th}}(g_{\text{bar}}, g_{\dagger})$  for the chi-squared (2), and employ the MCMC method to explore the entire parameter space  $\{A, B, l, b\}$ . We have no information about the dipole anisotropy, thus a flat prior for the parameter space is needed, which will be discussed in Section 4. Actually, the MCMC method used here is same as the maximum likelihood method, and the best-fit value corresponds to the minimal chi-squared ( $\chi_{\text{min}}^2 = -2 \ln \mathcal{L}_{\text{max}}$ ).

Second, we assume that the dipole anisotropy in radial acceleration is induced by spatial variation of the acceleration scale, which is a unique parameter in the radial acceleration relation. The acceleration scale with a monopole and dipole correction is of the form

$$\hat{g}_{\dagger} = g_{\dagger} (1 + C + D \hat{\mathbf{n}} \cdot \hat{\mathbf{p}}), \quad (5)$$

where the fiducial acceleration scale has also been fixed at the best-fit value  $g_{\dagger} = 1.02 \times 10^{-10} \text{ m s}^{-2}$ , and other parameters have analogous meanings with those in Eq. (4). Then we substitute the corrected acceleration scale (5) into the theoretical centripetal acceleration (3). By making use of  $g_{\text{th}}(g_{\text{bar}}, \hat{g}_{\dagger})$  for the chi-squared (2), we employ the MCMC method to explore the entire parameter space  $\{C, D, l, b\}$ . Finally we minimize the chi-squared to obtain the best-fitting value.

The monopole terms in both corrections are retained for complete description, but usually the monopole term is negligible. As a comparison, we repeat the above process with only the dipole term for both corrections. In total we have four corrections for the radial acceleration relation.

### 3.3 Model comparison

To assess the goodness of fit and take account of the number of free parameters in each model, we employ the information criteria (IC) to compare the corrected model i.e.  $\hat{g}_{\text{th}}(g_{\text{bar}}, g_{\dagger})$  or  $g_{\text{th}}(g_{\text{bar}}, \hat{g}_{\dagger})$  with the reference model  $g_{\text{th}}(g_{\text{bar}}, g_{\dagger})$ . Here the corrected model can degenerate to the reference model when the monopole term and the dipole magnitude both equal zero. The two most widely used information criteria are the Akaike information criterion (AIC) [35] and the Bayesian information criterion (BIC) [36]. They are defined as

$$\text{AIC} = \chi_{\text{min}}^2 + 2k, \quad (6)$$

$$\text{BIC} = \chi_{\text{min}}^2 + k \ln n, \quad (7)$$

where  $\chi_{\min}^2$  is the minimal chi-squared calculated by Eq. (2),  $k$  is the number of free parameters, and the total number of data points is  $n=2693$ . Differently from AIC, due to  $\ln 2693 > 2$ , the BIC heavily penalizes models with an excess of free parameters. Only the relative value of IC between different models is important in the model comparison. By convention, a model with  $\Delta\text{IC} > 5$  is regarded as ‘strong’ and  $\Delta\text{IC} > 10$  as ‘decisive’ evidence against a weaker model with higher IC value [37–39].

## 4 Results

We implement the MCMC method by using the affine-invariant Markov chain Monte Carlo ensemble sampler in emcee [40], which is widely used in astrophysics and cosmology. One hundred random walkers were used to explore the entire parameter space. We ran 500 steps in the burn-in phase and another 2000 steps in the production phase, which is enough for our pur-

pose. The dipole direction and its opposite direction give the same correction when the dipole magnitude changes its sign. To obtain an unambiguous result, we confined the dipole magnitude to be positive, and constrained the dipole direction to one cycle range, i.e.  $l \in [0^\circ, 360^\circ]$ ,  $b \in [-90^\circ, 90^\circ]$ . The MCMC method needs a prior distribution for each parameter but we do not have any information about the dipole anisotropy. In this paper, we adopt a flat prior distribution for each parameter as follows:  $A(C) \sim [-1, 1]$ ,  $B(D) \sim [0, 1]$ ,  $l \sim [0^\circ, 360^\circ]$ ,  $b \sim [-90^\circ, 90^\circ]$ .

The MCMC result for parameter space  $\{A, B, l, b\}$  is shown in Fig. 2. For every parameter, its distribution is almost Gaussian and the slightly larger one of  $1\sigma$  credible interval is regarded as its uncertainty. The  $\hat{g}_{\text{th}}$ -monopole term is  $A = -0.01 \pm 0.01$ . It is negligible. The  $\hat{g}_{\text{th}}$ -dipole magnitude is  $B = 0.10 \pm 0.01$ . It is a significant signal for anisotropy. The  $\hat{g}_{\text{th}}$ -dipole direction points towards  $(l, b) = (176.54^\circ \pm 7.55^\circ, -16.59^\circ \pm 5.11^\circ)$ . The MCMC result for another parameter space

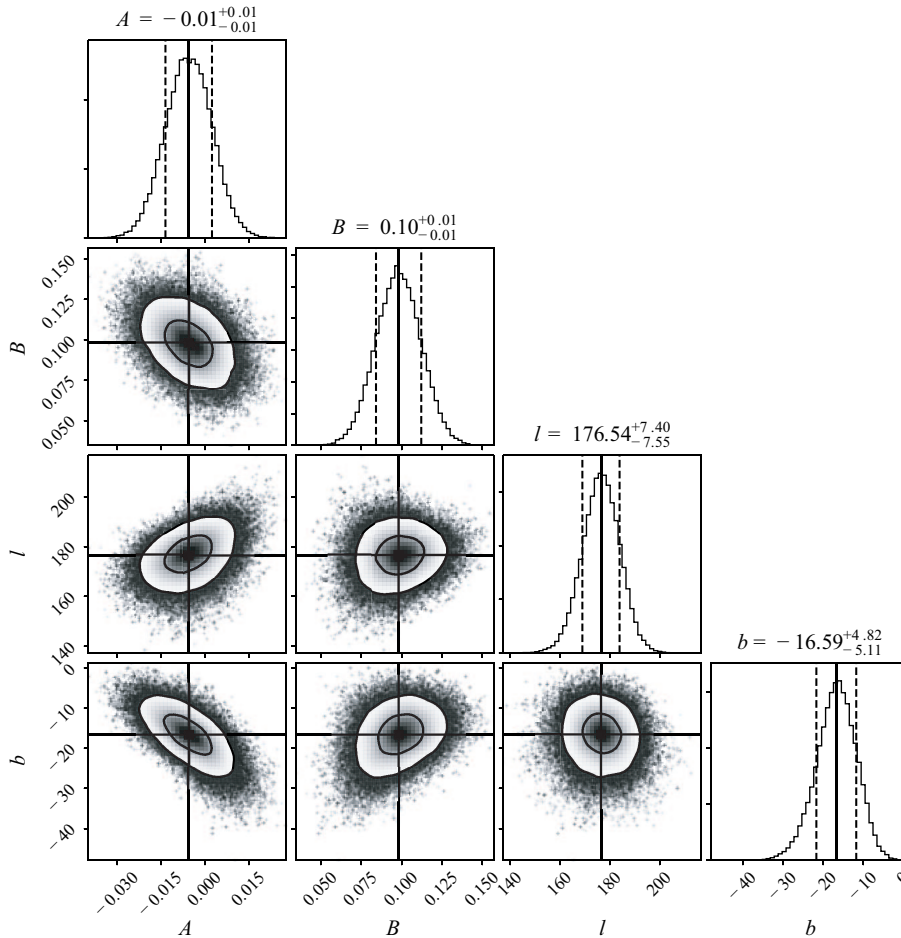


Fig. 2. The 1-dimensional marginalized histograms and 2-dimensional marginalized contours for the parameter space  $\{A, B, l, b\}$ . The horizontal and vertical solid lines mark the median values. The vertical dashed lines mark the  $1\sigma$  credible intervals. These values are labeled at the top of each histogram. The 2-dimensional marginalized contours mark  $1\sigma$ ,  $2\sigma$  credible regions from grey to light.

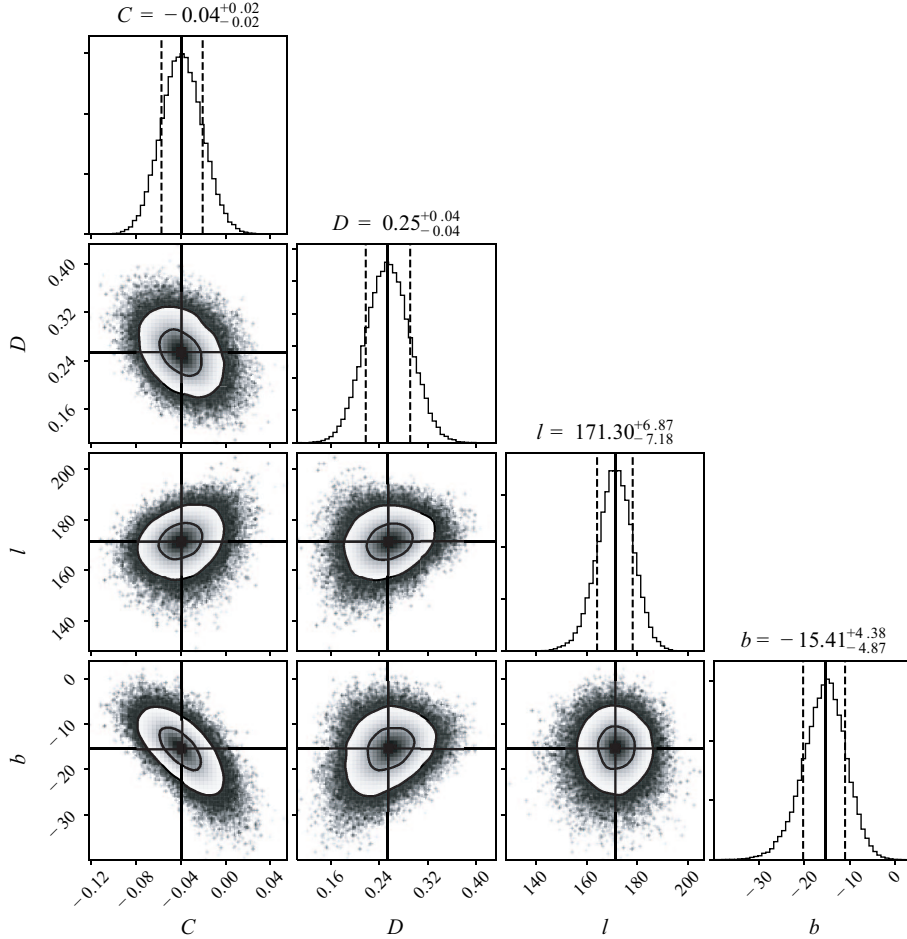


Fig. 3. The 1-dimensional marginalized histograms and 2-dimensional marginalized contours for the parameter space  $\{C, D, l, b\}$ . The horizontal and vertical solid lines mark the median values. The vertical dashed lines mark the  $1\sigma$  credible intervals. These values are labeled at the top of each histogram. The 2-dimensional marginalized contours mark  $1\sigma$ ,  $2\sigma$  credible regions from grey to light.

Table 1. The best-fit values with their  $1\sigma$  uncertainties for four dipole models. The unnormalized  $\chi^2$  for each correction, and the  $\Delta\text{AIC}$  values, which are against the reference model (3), are given in the last three columns.

model	$A(C)$	$B(D)$	$l$	$b$	$\chi^2$	$\Delta\text{AIC}$	$\Delta\text{BIC}$
$\hat{g}_{\text{th}}$ -dipole	$-0.01 \pm 0.01$	$0.10 \pm 0.01$	$176.54^\circ \pm 7.55^\circ$	$-16.59^\circ \pm 5.11^\circ$	3955	-59	-41
-	-	$0.09 \pm 0.01$	$178.96^\circ \pm 7.52^\circ$	$-18.84^\circ \pm 3.90^\circ$	3956	-60	-48
$\hat{g}_{\text{t}}$ -dipole	$-0.04 \pm 0.02$	$0.25 \pm 0.04$	$171.30^\circ \pm 7.18^\circ$	$-15.41^\circ \pm 4.87^\circ$	3962	-52	-34
-	-	$0.23 \pm 0.04$	$175.79^\circ \pm 8.14^\circ$	$-22.80^\circ \pm 4.29^\circ$	3967	-49	-37

$\{C, D, l, b\}$  is shown in Fig. 3. The same as Fig. 2, the distribution for each parameter is almost Gaussian. The  $\hat{g}_{\text{t}}$ -monopole term is  $C = -0.04 \pm 0.02$ . It is more significant than the  $\hat{g}_{\text{th}}$ -monopole term, but it is still negligible. The  $\hat{g}_{\text{t}}$ -dipole magnitude is  $D = 0.25 \pm 0.04$ . It is another significant signal for anisotropy. The  $\hat{g}_{\text{t}}$ -dipole term directly indicates that the acceleration scale could be spatially variable. The  $\hat{g}_{\text{t}}$ -dipole direction points towards  $(l, b) = (171.30^\circ \pm 7.18^\circ, -15.41^\circ \pm 4.87^\circ)$ .

The 2-dimensional marginalized contours for both parameter spaces have very similar shapes. In addition,

the two dipole directions are very close to each other, and the angular separation is only  $5.17^\circ$  (see Fig. 4). Furthermore, the minimal chi-squared of the  $\hat{g}_{\text{t}}$ -dipole model is close to that of the  $\hat{g}_{\text{th}}$ -dipole model (see Table 1). These results mean that the dipole anisotropy in the radial acceleration is mostly induced by the dipole anisotropy in the acceleration scale. In our previous work [26], we employed the hemisphere comparison method with the same SPARC data set to search for possible spatial anisotropy in the acceleration scale. We found the maximum anisotropy direction is pointing in the di-

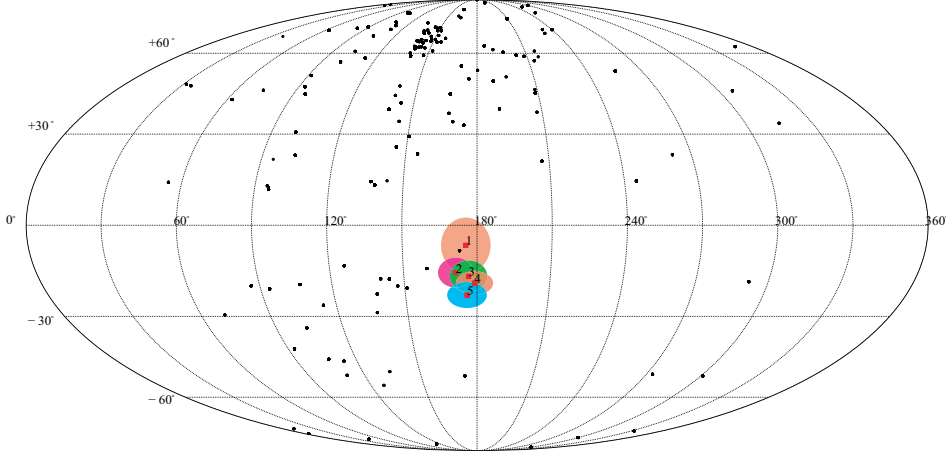


Fig. 4. (color online) The distribution of 147 SPARC galaxies on the sky (galactic coordinate system). Each point represents a single galaxy. The square points with confidence regions, labeled with numbers, represent the direction of the hemisphere anisotropy ( $2\sigma$ ) or dipole anisotropy ( $1\sigma$ ). Specifically, they are: 1) the hemisphere anisotropy; 2) the  $\hat{g}_\dagger$ -dipole anisotropy with monopole and dipole corrections; 3) the  $\hat{g}_{th}$ -dipole anisotropy with monopole and dipole corrections; 4) the  $\hat{g}_{th}$ -dipole anisotropy with dipole correction; and 5) the  $\hat{g}_\dagger$ -dipole anisotropy with dipole correction.

rection  $(l, b) = (175.5^{+6^\circ}_{-10^\circ}, -6.5^{+9^\circ}_{-3^\circ})$ , which is very close to the  $\hat{g}_\dagger$ -dipole direction, and the angular separation is only  $9.82^\circ$  (see Fig. 4).

For both the dipole models, the monopole term is indeed negligible compared to the dipole magnitude, so we can neglect it from both corrections. Table 1 is the MCMC result for all dipole models with or without the monopole term. Without the monopole term, both dipole magnitudes become slightly smaller, and the dipole directions are both shifted a little to the southeast, with an angle less than  $8.52^\circ$  (see Fig. 4). In addition, the chi-squares also have a slightly increase. These results indicate that the monopole term only has a slight impact on the dipole anisotropy. Both AIC and BIC indicate that there is ‘decisive’ evidence for all dipole models against the reference model, but it is indistinguishable from the dipole model with or without the monopole term. Even though there is ‘strong’ evidence for the  $\hat{g}_{th}$ -dipole model against  $\hat{g}_\dagger$ -dipole model, these models could be compatible when the dipole anisotropy in radial acceleration is induced by the dipole anisotropy in acceleration scale.

## 5 Monte Carlo simulations

As a robust check, we examined whether the dipole anisotropy could be derived from statistical isotropy. First we created a mock data set from the SPARC data set. The dynamic centripetal acceleration  $g_{obs}$  is replaced by a random number which has a Gaussian distribution, i.e.  $G(g_{th}, \sigma_{obs})$ . Here  $g_{th}$  is the theoretical centripetal acceleration (3) and the acceleration scale has been fixed at the best-fit value  $g_\dagger = 1.02 \times 10^{-10} \text{ m s}^{-2}$ .  $\sigma_{obs}$  is the uncer-

tainty in  $g_{obs}$ . Except for the dynamic centripetal acceleration, other data, including the galactic coordination, acceleration uncertainties and the baryonic acceleration, remained unchanged. Then we employed the monopole and dipole corrections (4) and (5) for the radial acceleration relation with the mock data set and used the MCMC method to explore the entire parameter space  $\{A, B, l, b\}$  and  $\{C, D, l, b\}$ .

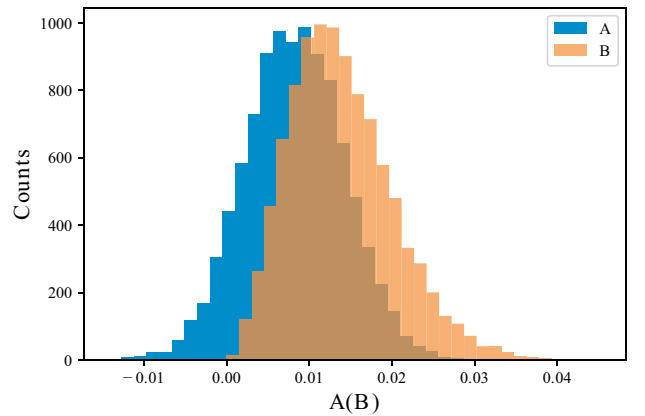


Fig. 5. (color online) The monopole term  $A$  and the dipole magnitude  $B$  in the isotropic mock data set for 10000 Monte Carlo simulations.

For both the dipole models, we find that it is hard to constrain the dipole direction. It has a relatively large uncertainty and spans in all possible directions. The monopole term is still negligible, but the dipole magnitude becomes much less than that from the SPARC data set. Figures 5 and 6 show the results of 10000 simulations for the  $\hat{g}_{th}$ -dipole model and  $\hat{g}_\dagger$ -dipole model (here

we use only the ODR algorithm to fit the radial acceleration relation, on account of the computation time). For the  $\hat{g}_{\text{th}}$ -dipole model, the monopole term centers on  $\bar{A} = 0.01$ . It rarely reaches  $A_{\text{max}} = 0.03$ , so that the monopole term is still negligible. The dipole magnitude centers on  $\bar{B} = 0.01$ , and its upper limit only reaches  $B_{\text{max}} = 0.04$ . It is much less than the dipole magnitude from the SPARC data set. For the  $\hat{g}_{\text{r}}$ -dipole model, the monopole term centers on  $\bar{C} = 0.01$ . It rarely reaches  $C_{\text{max}} = 0.07$ , so that the monopole term is still negligible. The dipole magnitude centers on  $\bar{D} = 0.03$ , and its upper limit only reaches  $D_{\text{max}} = 0.10$ . It is much less than the dipole magnitude from the SPARC data set. All these results mean that the dipole anisotropy from the original SPARC data set could not be reproduced by the isotropic mock data set. This check is consistent with the robust check for the hemisphere comparison method [26].

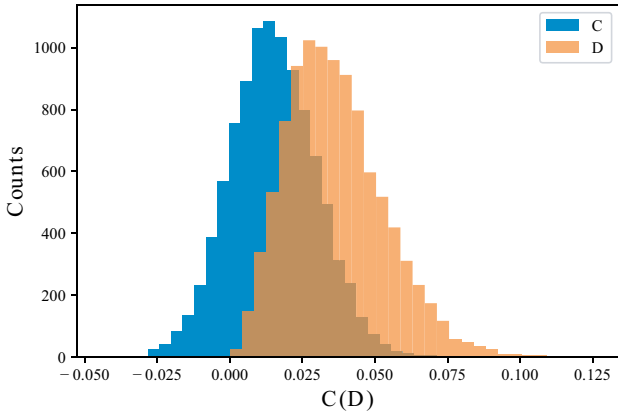


Fig. 6. (color online) The monopole term  $C$  and the dipole magnitude  $D$  in the isotropic mock data set for 10000 Monte Carlo simulations.

## 6 Discussion and conclusions

In this paper, we have shown the monopole and dipole correction for the radial acceleration relation with 147 rotationally supported galaxies. We found that there exists a significant dipole anisotropy in the radial acceleration, which is most probably induced by dipole anisotropy in the acceleration scale. The  $\hat{g}_{\text{r}}$ -dipole magnitude is significant and reaches  $D = 0.25 \pm 0.04$ . The  $\hat{g}_{\text{r}}$ -dipole direction is pointing in the direction  $(l, b) = (171.30^\circ \pm 7.18^\circ, -15.41^\circ \pm 4.87^\circ)$ , which is very close to the maximum anisotropy direction from the hemisphere comparison method. The monopole term is negligible. It only has a slight impact on the dipole anisotropy. The same as the hemisphere comparison method, a robust check has been made to examine the significance of the dipole anisotropy. The result shows that the dipole

anisotropy cannot be reproduced by an isotropic mock data set.

As pointed out in the introduction, the cosmological principle has been challenged by some cosmological observations. In this paper, we have found a possible dipole anisotropy in the acceleration scale  $g_{\text{r}}$  in the local Universe. The dipole direction is very close to the cosmological preferred direction from the hemisphere comparison method [26]. In addition, we find that the dipole direction in this paper is close to some other cosmological preferred directions. For instance, the anisotropy of cosmic acceleration [41] from Type Ia supernovae has been found to have a dipole direction  $(l, b) = (187.0^\circ, -18.8^\circ)$ , which is close to our dipole direction, with an angular separation of only  $15.38^\circ$ . Another dipole direction is from the spatial variation of the fine structure constant [9, 10], and it only has an angular separation of  $35.37^\circ$ . All these preferred directions hint that the Universe may be anisotropic, which could be related to some underlying physical effects, such as spacetime anisotropy [42–44]. If the cosmological principle is no longer valid, the standard  $\Lambda$ CDM model needs to be modified. However, it is still premature to claim that the Universe is anisotropic, due to the small data samples and the uncertainty in the current observations.

There are still some uncertainties in the original SPARC data set. As stated by McGaugh et al. [29], near-infrared (NIR) luminosity was observed, while physics requires stellar (baryonic) mass. The mass-to-light ratio  $\Upsilon_*$  is an unavoidable conversion factor which can be estimated by the stellar population synthesis (SPS) model [45]. The SPS model suggests that  $\Upsilon_*$  is nearly constant in the NIR (within  $\sim 0.1$  dex), thus McGaugh et al. [29] assume a constant  $\Upsilon_*$  for all galaxies to fit the radial acceleration relation. We use the same assumption in this paper as a precondition to search for the possible dipole anisotropy. Recently, Li et al. [46] took  $\Upsilon_*$  as ‘free’ parameter to fit the radial acceleration relation to individual SPARC galaxies. If the possible small variation of  $\Upsilon_*$  is taken into account, then the possible dipole anisotropy on acceleration scale may be impacted. Further investigations are necessary to seek possible degeneracy. Another possible uncertainty comes from the inhomogeneous distribution of galaxies in the sky (see Fig. 4). For future research on anisotropy with galaxies, it would be better to cover the sky homogeneously.

*We are grateful to Dr. Yu Sang and Dong Zhao for useful discussions. We are also thankful for the open access of the SPARC data set.*

## References

- 1 S. Weinberg, *Cosmology*, (Oxford, UK: Oxford University Press, 2008)
- 2 C. L. Bennett et al (WMAP), *Astrophys. J. Suppl.*, **208**: 20 (2013)
- 3 G. Hinshaw et al (WMAP), *Astrophys. J. Suppl.*, **208**: 19 (2013)
- 4 P. A. R. Ade et al (Planck), *Astron. Astrophys.*, **571**: A16 (2014)
- 5 P. A. R. Ade et al (Planck), *Astron. Astrophys.*, **594**: A13 (2016)
- 6 D. Hutsemekers, R. Cabanac, H. Lamy, and D. Sluse, *Astron. Astrophys.*, **441**: 915 (2005)
- 7 A. Kashlinsky, F. Atrio-Barandela, H. Ebeling, A. Edge, and D. Kocevski, *Astrophys. J.*, **712**: L81 (2010)
- 8 H. A. Feldman, R. Watkins, and M. J. Hudson, *Mon. Not. Roy. Astron. Soc.*, **407**: 2328 (2010)
- 9 J. K. Webb, J. A. King, M. T. Murphy, V. V. Flambaum, R. F. Carswell, and M. B. Bainbridge, *Phys. Rev. Lett.*, **107**: 191101 (2011)
- 10 J. A. King, J. K. Webb, M. T. Murphy, V. V. Flambaum, R. F. Carswell, M. B. Bainbridge, M. R. Wilczynska, and F. E. Koch, *Mon. Not. Roy. Astron. Soc.*, **422**: 3370 (2012)
- 11 A. Mariano and L. Perivolaropoulos, *Phys. Rev. D*, **86**: 083517 (2012)
- 12 Z. Chang, X. Li, H.-N. Lin, and S. Wang, *Eur. Phys. J. C*, **74**: 2821 (2014)
- 13 Z. Chang and H.-N. Lin, *Mon. Not. Roy. Astron. Soc.*, **446**: 2952 (2015)
- 14 H.-N. Lin, X. Li, and Z. Chang, *Mon. Not. Roy. Astron. Soc.*, **460**: 617 (2016)
- 15 V. C. Rubin, W. K. Ford, Jr., and N. Thonnard, *Astrophys. J.*, **225**: L107 (1978)
- 16 A. Bosma, *Astron. J.*, **86**: 1825 (1981)
- 17 A. Tan et al (PandaX-II), *Phys. Rev. Lett.*, **117**: 121303 (2016)
- 18 E. Aprile et al (XENON100), *Phys. Rev. D*, **94**: 122001 (2016)
- 19 M. Milgrom, *Astrophys. J.*, **270**: 365 (1983)
- 20 M. Milgrom, *New Astron. Rev.*, **46**: 741 (2002)
- 21 M. Milgrom, *Mon. Not. Roy. Astron. Soc.*, **437**: 2531 (2014)
- 22 K. G. Begeman, A. H. Broeils, and R. H. Sanders, *Mon. Not. Roy. Astron. Soc.*, **249**: 523 (1991)
- 23 R. A. Swaters, R. H. Sanders, and S. S. McGaugh, *Astrophys. J.*, **718**: 380 (2010)
- 24 Z. Chang, M.-H. Li, X. Li, H.-N. Lin, and S. Wang, *Eur. Phys. J. C*, **73**: 2447 (2013)
- 25 M. Milgrom, in *Proceedings, 2nd International Heidelberg Conference on Dark matter in astrophysics and particle physics (DARK 1998): Heidelberg, Germany, July 20-25, 1998* (1998) p. 443-457
- 26 Y. Zhou, Z.-C. Zhao, and Z. Chang, *Astrophys. J.*, **847**: 86 (2017)
- 27 F. Lelli, S. S. McGaugh, and J. M. Schombert, *Astron. J.*, **152**: 157 (2016)
- 28 <http://astroweb.cwru.edu/SPARC/>
- 29 S. S. McGaugh, F. Lelli, and J. M. Schombert, *Phys. Rev. Lett.*, **117**: 201101 (2016)
- 30 A. Begum and J. N. Chengalur, *Astron. Astrophys.*, **424**: 509 (2005)
- 31 W. J. G. de Blok, S. S. McGaugh, and J. M. van der Hulst, *Mon. Not. Roy. Astron. Soc.*, **283**: 18 (1996)
- 32 <http://ned.ipac.caltech.edu/>
- 33 M. Milgrom, (2016), arXiv:1609.06642
- 34 P. T. Boggs, R. H. Byrd, and R. B. Schnabel, *SIAM Journal on Scientific and Statistical Computing*, **8**: 1052 (1987)
- 35 H. Akaike, *IEEE Transactions on Automatic Control*, **19**: 716 (1974)
- 36 G. Schwarz, *Annals of Statistics*, **6**: 461 (1978)
- 37 A. R. Liddle, *Mon. Not. Roy. Astron. Soc.*, **377**: L74 (2007)
- 38 F. Arevalo, A. Cid, and J. Moya, *Eur. Phys. J. C*, **77**: 565 (2017)
- 39 H.-N. Lin, X. Li, and Y. Sang, (2017), arXiv:1711.05025
- 40 D. Foreman-Mackey, D. W. Hogg, D. Lang, and J. Goodman, *Publications of the Astronomical Society of the Pacific*, **125**: 306 (2013)
- 41 W. Zhao, P.-X. Wu, and Y. Zhang, *Int. J. Mod. Phys. D*, **22**: 1350060 (2013)
- 42 Z. Chang, S. Wang, and X. Li, *Eur. Phys. J. C*, **72**: 1838 (2012)
- 43 Z. Chang, M.-H. Li, and S. Wang, *Phys. Lett. B*, **723**: 257 (2013)
- 44 X. Li, H.-N. Lin, S. Wang, and Z. Chang, *Eur. Phys. J. C*, **75**: 181 (2015)
- 45 J. M. Schombert and S. McGaugh, *PASA*, **31**: e011 (2014)
- 46 P.-F. Li, F. Lelli, S. McGaugh, and J. Schombert, *Astron. Astrophys.*, **615**: A3 (2018)